

The CMS Outer HCAL SiPM Upgrade

Artur Lobanov for the CMS Collaboration

Deutsches Elektronen-Synchrotron, Notkestrasse 85, D-22607 Hamburg

E-mail: artur.lobanov@desy.de

Abstract. The CMS Outer Hadron Calorimeter (HO) is the first large scale hadron collider detector to use SiPMs. By late January 2014 the installation of 1656 of 2376 channels was completed. The HO readout system provides for active temperature stabilization of the SiPMs to less than 0.1°C using Peltier coolers, temperature measurement, and software feedback. Each channel has independently controlled bias voltage with a resolution of 25 mV. Each SiPM is read out by 40 MHz QIE ADCs. We report on the system design, schedule and progress. The next phase for the detector is commissioning during 2014 before the 2015 LHC run. We report on the status of commissioning and plans for operation. We discuss the calibration strategy with local cosmic ray runs using the HO's self trigger ability. We discuss the plans for a global CMS operations run in November 2014.

1. The CMS Hadron Outer Calorimeter

The CMS central hadron calorimeter is a sampling calorimeter with brass absorber and plastic scintillator tiles with wavelength shifting fibers. The barrel hadron (HB) calorimeter is complemented with an outer calorimeter (HO) located just outside the cryostat and inside the magnetic flux return yoke [1]. It provides an additional calorimeter coverage of about 3λ thickness and ensures containment of highly energetic hadron showers, thus it works as a tail-catcher to improve the energy measurement of jets and missing transverse energy [2].

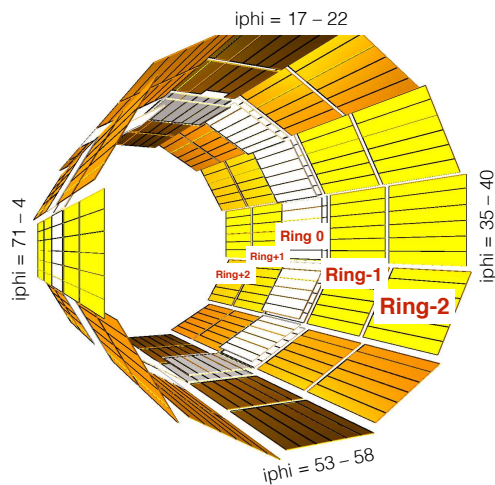
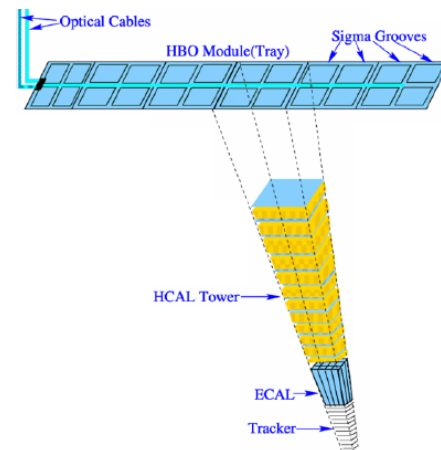
The HO is located in all 5 barrel rings of CMS and is split into 30 sections (η) along the Z-axis (beam-pipe). In the transverse plane, the HO consists of 12 sectors, each with 6 trays, totalling 72 sections (ϕ), each 5° . The HO tiles contain two layers of scintillator in the central ring of the detector, and one layer everywhere else (see Fig. 1). The scintillation light is collected with wavelength shifting fibers and transmitted over clear fibers to front-end electronics placed close to the layers. Each ϕ - η position is read out by a separate channel, summing to 2160 physical channels. A schematic layout of the calorimeters in CMS and the location of the HO scintillators is shown in Fig. 2. The tile size is chosen to match projective towers in the HB.

In addition, some readout channels are not connected to any scintillator and can be used for noise measurements and calibration. The total number of active electronics channels is 2376.

In the original design the wavelength shifted scintillator light was read out by hybrid photo diodes (HPDs). However, during operation in CMS they proved to be sub-optimal in the run conditions for several reasons:

- Discharge caused by the fringe field of the CMS magnet.
- Low gain and photo detection efficiency.
- Ageing.



**Figure 1.** HO layout**Figure 2.** HO tiles corresponding to HB towers

The CMS HCAL group developed a drop-in replacement for the current front-end based on silicon photo multipliers (SiPMs) as photo-sensors [3]. The main advantages of SiPMs are the magnetic field insensitivity, relatively high photon-detection efficiency, and high gain. Also SiPM boards could easily fit into the limited space of the existing readout modules. In this configuration each eta-phi segment is readout by a single SiPM corresponding to a single electronics channel.

This upgrade design has been validated using laboratory measurements, test-beam data, and on the detector itself. The upgrade took place during the first LHC long shutdown in 2013-2014 - first, the existing readout modules (RM) were extracted from the detector, then, they were refurbished with SiPMs, and burned-in in a test stand. After verifying that the RMs were working properly, they were installed in CMS. Additionally, during the installation the commissioning of the upgraded parts began.

2. Commissioning

Primary reasons for commissioning during the installation are to identify problems with the new and existing hardware, to validate the installation, and, in case of malfunctions, to make repairs. This is of critical importance, as the barrel part of CMS will be closed until the next extensive upgrade.

The first commissioning step is a communication test with the readout system and the verification of slow control operation and channel response. Then, the measurement and optimization of SiPM operational variables is done as follows:

2.1. Temperature

The SiPM gain depends linearly on the temperature with a relative dependence of 8% gain shift per °C at a foreseen operating point of 1.5 V over-voltage [4]. This temperature dependence requires active control of the temperature of the SiPM with better than 0.1°C stability. Therefore, the SiPM temperature is stabilized by a Peltier element mounted on the back of the SiPM mounting board.

Instead of operating all SiPMs at the same temperature, it was chosen to fix the Peltier voltage at around 0.3 V. This minimizes the power consumption while providing a large range of cooling options.

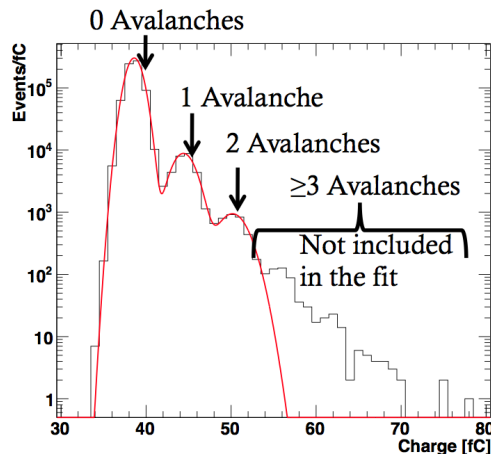


Figure 3. Pedestal spectrum of a SiPM with the gain fit

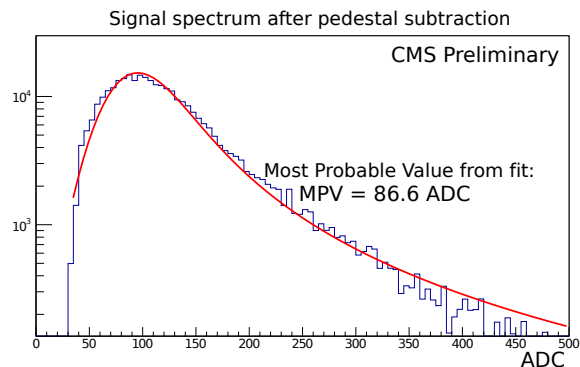


Figure 4. Single channel pedestal subtracted signal spectrum with coincidence trigger

2.2. Gain

The SiPM gain is adjusted by the operating voltage and can be measured from the single photo electron (SPE) spectrum as in Fig. 3. The distance between the SPE peaks (avalanches) is gain. All channels are set up to have gain around 6 ADC counts/photo-electron to prevent the ADC from saturation, but still have a good signal-to-noise ratio.

2.3. Pedestal

The SiPM signal is digitized corresponding to the LHC clock in 25 ns time-slices (TS), so this is the basic signal element from the ADC. To have a uniform response from all channels, the pedestal is set to 9 ADC counts per 1 TS. For a 4 TS sum, which is used in HO, this results in ≈ 36 ADC counts (0 avalanches in Fig. 3).

2.4. LED

An LED system is used to monitor the stability of the SiPMs outside of collisions. To adjust it to the new photo sensor type, an LED light calibration is performed. Because of different SiPM-fiber light coupling in Ring 0 and Rings 1-2, the LED amplitude is set to different values.

After the successful completion of these commissioning steps, the new readout hardware is ready for data taking.

3. Cosmic analysis

Cosmic runs with HO data is the verification of installation and operation of the new readout electronics. Additionally, an initial muon calibration can be obtained by extracting the MIP signal values of all channels.

Despite the location of the CMS detector, approximately 100 m below the surface, in certain parts of the underground cavern a 20 m wide access shaft allows a higher muon flux. During the long shutdown, some of the CMS rings are placed in different positions including under the shaft. This biases the occupancy of the different scintillator tiles, but gives a high rate and yielding a higher statistics.

In contrast to global CMS runs which include data from its muon detector systems, the events for this analysis are taken locally, meaning only HO data is read out with the HO trigger. The HO trigger is setup as follows: each wheel with 12 sectors is split into 4 quadrants of 3 sectors each; a technical trigger processor constantly monitors for firing channels over a threshold of

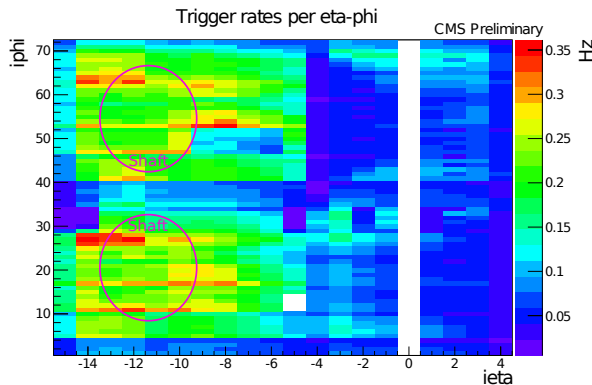


Figure 5. Trigger rate of each individual channel.

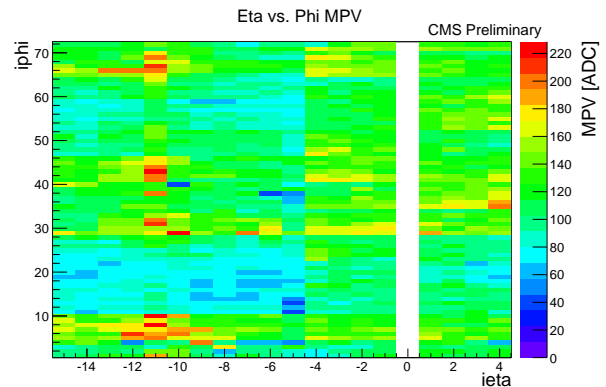


Figure 6. Landau fit most probable values (MPV) of individual channels

40 fC in 1 TS; if two channels from different quadrants are above threshold the trigger fires and the event is written to a disk. A time delay of 1 TS between the top and bottom quadrants is required to account for the time of flight through a diameter of approximately 8 m.

Trigger rates of all individual HO channels, obtained with this coincidence trigger configuration, are shown in figure 5. At the time of data taking, only 3 rings covering $i\eta$ -15 to +4 had been upgraded with SiPMs, but the $i\eta = 0$ white stripe is due to HCAL coordinate system and not a physical gap in the detector. The empty spot at $i\eta = -5$ corresponds to the magnet chimney, where HO is not instrumented.

The highest rates are observed in the horizontal tiles ($i\phi = 15-25, 55-65$) in the wheels under the shaft (YB-2: $i\eta = -15, -11$; YB-1: $i\eta = -10, -5$). The gap between the moving wheels and the central YB0 ($i\eta = -4, 4$) is more than 5 m, so the drop in the rate around the edge at $i\eta = -5$ is considerably high. The fine structure of outliers along $i\phi$ lines is due to the different scintillator tiles sizes, which also leads to different light collection efficiencies. So $i\eta = -15$ shows lower rates because these tiles are half as big as the neighbours.

3.1. Muon calibration

For the muon calibration, the MIP value for each channel had to be extracted. Theoretically, a MIP would give a Landau signal distribution for a thin layer, but because of the thickness of the scintillator the signal is smeared. Each channel's pedestal subtracted signal spectrum (where the signal is summed over 4 TS = 100 ns) is fitted with a Landau⊗Gauss convoluted function and the most probable value (MPV) is taken as the MIP value. In case of noise contamination in the signal region, the tail is fitted with an exponential to improve the signal fit.

Figure 6 shows the MPV values for all individual HO channels. The MPV values are not uniform due to several factors:

- Ring 0 has 2 scintillator layers, while rings 1 and 2 have 2 layers.
- Altered light coupling of the fibers to the SiPMs in different rings.
- Different sizes of the scintillators lead to varying light detection efficiency.
- Fibers connecting SiPMs and tiles vary in length depending on the distance between scintillator and readout module. For YB-1,2 the readout is located between these rings (between $i\eta = -11, -10$) and for YB0 it is on both edges of the ring ($i\eta = \pm 4$).
- Variation in $i\phi$ because of sector alignment and cosmic ray muon track path-length in the scintillator (track vs. tile angle): the lowest MPVs are measured at top and bottom tiles.

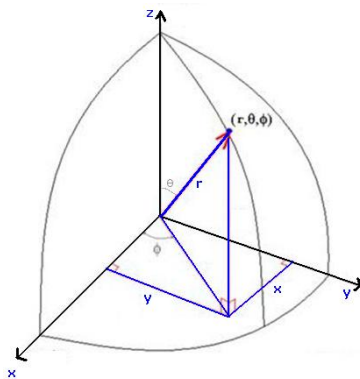


Figure 7. x and y are coordinates of the muon track vector projection on the horizontal plane. $x, y = 0$ corresponds to a vertical muon

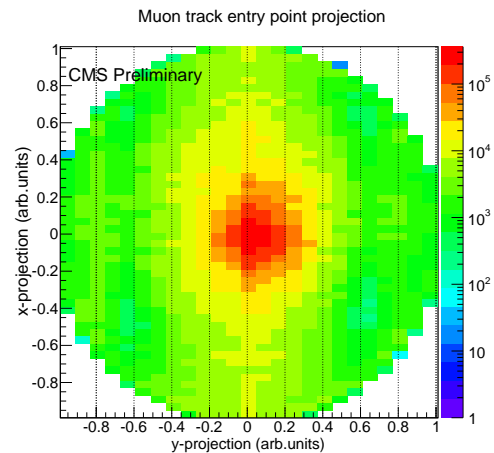


Figure 8. HO Muon entry point (as in Fig. 7) shifted because of shaft

The last variation is not hardware related, and causes a bias in the MIP value estimation as the calibration is performed for muons passing the tile perpendicular to it. The signal distribution is smeared and shifted towards higher values and, as each muon has a unique incident angle, the path-length correction has to be applied for each event. Therefore a signal correction algorithm has been developed. For each event the muon track is built using only two HO hits, and the angles between the track and the two scintillator planes are calculated. Then the recorded signal is multiplied by the cosine of this angle to get the value a normal muon would give in the tile.

The spatial distribution of the HO muon tracks in Fig. 8 shows a good reconstruction performance and agrees with the cavern layout.

Figure 9(a) shows the signal spectra with and without path-length correction for a side tile of HO, which has a large angle to the abundantly vertical muons coming from the sky. As expected, the uncorrected distribution is shifted to higher values and broader, than the corrected one. In

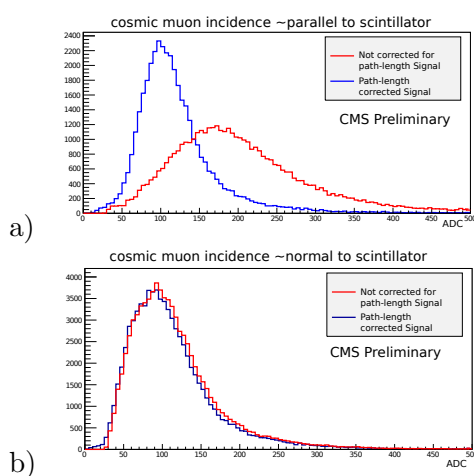


Figure 9. Signal spectra for side (a) and top (b) tiles with and without muon path-length correction

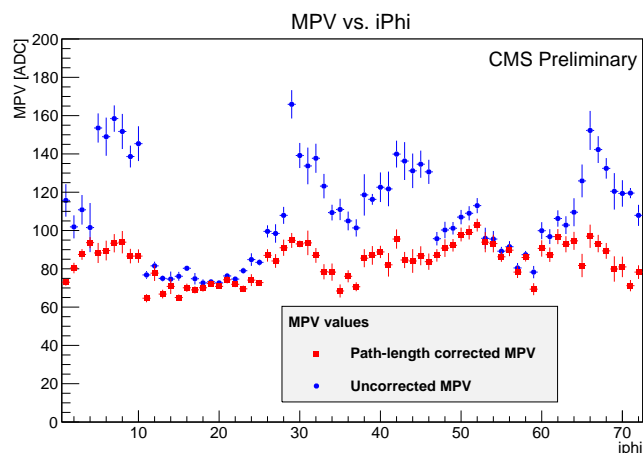


Figure 10. Averaged over YB-1,2 MPV profile along $i\phi$

contrast, for a horizontally aligned tile, which is mostly hit normally by muons, the path-length correction doesn't introduce any visible shift as seen in Fig. 9b.

After the correction, the MPV values of different channels become more equal (compare blue histograms in Fig. 9 (a) and (b) with the remaining variation coming from hardware differences. Figure 10 shows an averaged profile of the MPV values before and after muon path-length correction. The average is taken for the rings -1 and -2 as these have the highest statistics due to the position under the access shaft. In the blue profile a modulation is seen which corresponds to the alignment of the HO sectors forming a circle. The correction flattens out the general modulation, but leaves local variations, which are related to the hardware.

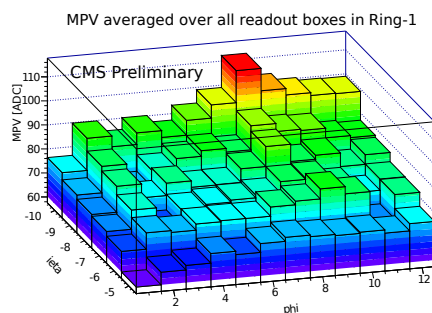


Figure 11. HO trigger layout

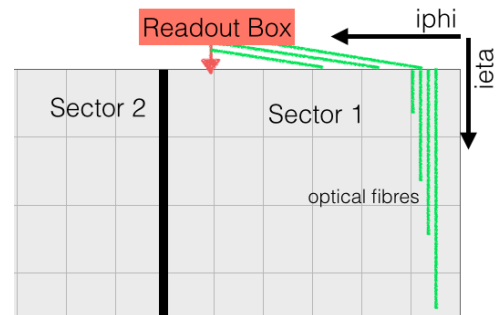


Figure 12. HO detector layout

A source of this remaining signal variation is the fiber light attenuation. From the cabling point of view, all sectors within a wheel are symmetric and should show the same behaviour of MPV variation with respect to the scintillator-SiPM distance. In rings -1 and -2 each readout box is connected to 12 iphi trays. Figure 11 shows the average MPV values over all readout boxes of ring -1 corresponding to ieta -10,-5. One can clearly see the location of the readout modules with SiPMs (where the distance to the tiles is the minimal) and the decrease to the sides.

The decrease along ieta is due to the cable length inside the scintillator tray, and along phi the MPV decreases with the length of the fibers connecting the trays with the readout boxes (see Fig. 12).

4. Summary

The CMS outer hadronic calorimeter is being upgraded with SiPMs during the first long shutdown of the LHC. The installed new readout is successfully commissioned and optimized for operation. A validation of the installation and calibration with cosmic muons is shown to be possible with an HO only trigger setup. Given the detector configuration, the obtained muon calibration is in agreement with the expectations from test-beam data.

As of April 2014 the whole HO detector is upgraded and commissioned. A global run with the CMS muons systems is planned for November 2014, and after the relaunch of the LHC in 2015, calibration with pp-collision data will become possible. The performance of the upgraded HO will allow the CMS RPC muon system to use HO data for a combined muon trigger.

References

- [1] CMS Hadron Calorimeter Technical Design Report., CERN/LHCC 97-31, CMS TDR 2, June 20th, 1997
- [2] Abdullin S et al. (CMS Collaboration) 2008, *Eur. Phys. J.* **C57** 653-663
- [3] Lutz B et al. (CMS Collaboration) 2012, *J. Phys.: Conf. Ser.* **404** 012018
- [4] Anderson J et al. (CMS Collaboration) 2012, *Phys. Procedia* **37** 72 -78